



## A Novel Application for Parabolic Trough Solar Collector Based on Helical Receiver Tube and Nano-Fluid with a Solar Tracking Mechanism

Saad T. Hamidi <sup>a\*</sup>

<sup>a</sup> Electromechanical Eng. Dep., University of Technology, Baghdad, Iraq. [saadtami@yahoo.com](mailto:saadtami@yahoo.com)

\* Corresponding author.

Submitted: 28/07 /2019

Accepted: 13/12 /2019

Published: 25/05/2020

### KEY WORDS

Parabolic trough solar collector, helical coil tube, Nano-fluids, tracking mechanism, thermal efficiency

### ABSTRACT

*Novel techniques to enhance thermal performance using a helical coil receiver tube and Nano-fluid materials are presented in this paper. Two different applied techniques to enhance thermal performance are used as a new application on parabolic trough solar collector (PTSC). In the present work, PTSC has been fabricated using Dioxide Silicon SiO<sub>2</sub> with an average particle size of 40nm by taking volume fraction of SiO<sub>2</sub> 0.1, 0.2 and 0.3%. Distilled water based Nano-fluid as a working fluid and a helical coil receiver tube were used in this paper. Varying the flow rate of Nano-fluids 100,150 and 200l/h are used, respectively. A solar tracking mechanism experimentally has been used with the PTSC. As per ASHRAE standard, the experimental results showed that at volume fraction 0.3 % and flow rate of 200 l/h, the highest increase in the energy absorbed factor  $FR(\tau\alpha)$  was 14.6 % and energy removal factor  $F_{RUL}$  was 29.4 % compared with distilled water. The changes in  $F_{R(\tau\alpha)}$  vary from 11.8% to 14.6% while in  $F_{RUL}$ , they vary from 20.5% to 29.4% as compared with the distilled water case. The maximum efficiency was about 76.6 % as the heat loss parameter  $[(T_i - T_o)/G_T] = 0$  at a volume fraction of 0.3 % and the flow rate of 200 l/h.*

**How to cite this article:** Saad. T. Hamidi, "A novel application for parabolic trough solar collector based on helical receiver tube and nano-fluid with a solar tracking mechanism," *Engineering and Technology Journal*, Vol. 38, Part A, No. 05, pp. 656-668, 2020.

DOI: <https://doi.org/10.30684/etj.v38i5A.496>

This is an open access article under the CC BY 4.0 license <http://creativecommons.org/licenses/by/4.0>.

### 1. Introduction

The use of solar energy is a promising option for addressing many energy and environmental problems [1,2]. Solar concentrating collectors are capable of producing beneficial heat at moderate and heightened levels. The PTSC are most common concentrating techniques and they could be invested in numerous applications such as power production, thermal solar, desalination, solar photocatalysis system [3,4]. In recent years, much research has focused on different ways to enhance thermal performance (PTSC) in order to use a more useful heat tube. In general, the aim of these mechanisms is to raise the coefficient of heat transfer in the flow for achieving advantageous conditions of that flow [5]. These topologies could be divided into two broad classes; using the

geometry of PTSC or utilizing the different fluids [6]. The first class, utilizes the black coating tubes [7], internal insert fins [8-9], and flow inserts [10] as the most common topologies. Those topologies are trying to raise the heat transfer between the absorber receiver tube and the fluid to be enhanced. The different empirical studies have pointed out that helically coiled tube heat exchangers are extremely helpful due to its spiral coil form which introduces better flow in minimum space and larger heat transfer area [11]. This composition yields a higher the coefficient of heat transfer when compared to the straight tube heat exchanger under the same empirical conditions. A complex flow pattern is generated within the helical tube will lead to enhancement in the rate of heat transfer [12]. The researcher [13] had compared the result the computation of fluid dynamic (CFD) of the straight tube and helical coil tube heat and exchanger using the same length, identical operating conditions. The result showed ,the rate of heat transfer is rising 11% showed that the rate of heat transfer of helical coil heat exchanger rising 11% and 10% in the Nussle number compared to straight tube. Investigated the impact of geometrical and operational factors on the thermal efficiency of helical coil and shell tube heating exchangers [14]. The analysis was implemented at uniform state. Water as working fluid was used for both sides, whereas its viscosity and thermal conductivity and viscosity were supposed depending on temperature. Depending on obtained findings, two relations to forecasting the thermal impact at extensive ranges of flow rate ratios, the product of Reynolds numbers, and dimensionless geometrical parameters. At the same values of capacity ratio and number of transfer units, it was found that the effectiveness is averagely decreased by 12.6% with respect to the parallel flow heat exchangers with an approximately constant difference. Studied two heat exchangers, representing by straight tube and helical coil tube, by adding nanoparticles like  $\text{TiO}_2$  and  $\text{SiO}_2$  with the employed fluid [15]. The heat exchanger of helically coiled heat had been tested and analysed based on the difference mean temperature, Reynolds number and coefficient of heat transfer. It is conducted from the collected results that the helical coil exchangers become more efficient by adding the nanoparticles in the employed working fluid as well as its overall heat transfer coefficient. Also, using Nano-fluids as work fluids is another more common topology. The Nano-fluids is composed of metal or non-metal nanoparticles dispersed in the base fluid as proposed [16]. The basic thought of using Nano-fluid is to raise the fluid thermal connectivity since the thermal conductivity of the nanoparticles is several times higher than basic fluids, usually thermal oil or distilled-  $\text{H}_2\text{O}$  [17]. Using the Nano-fluids extensively has been exploiting in the literature by several researchers. Table 1 contains various empirical research studies [18-24] and investigates different types of Nano-fluid in PTSC.

**Table 1: Literature of some few experimental studies Nano-fluid-based PTSC**

Experimental study	Base fluid	Nano-Particles	Enhancement % of thermal efficiency $\eta$	Methods	Ref
Sunil et al. 2014	Distilled- $\text{H}_2\text{O}$	$\text{SiO}_2$ , $\text{CuO}$	6.17 at 0.05% vol.con. 12.49 at 0.05% $\text{CuO}$	Exp.	[18]
Chaudhari et al. 2015	Distilled- $\text{H}_2\text{O}$	$\text{Al}_2\text{O}_3$	7 at 0.1% vol.con	Exp.	[19]
Subramani et al. 2017	Distilled- $\text{H}_2\text{O}$	$\text{Al}_2\text{O}_3$	8.54	Exp.	[20]
Rehan et al. 2018	Distilled- $\text{H}_2\text{O}$	$\text{Al}_2\text{O}_3$ , $\text{Fe}_2\text{O}_3$	13, 11	Exp.	[21]
Subramani et al. 2018	Distilled- $\text{H}_2\text{O}$	$\text{TiO}_2$	8.66	Exp.	[22]
Deep et al. 2018	Distilled- $\text{H}_2\text{O}$	$\text{TiO}_2$	8.56 at 0.75% vol.con	Exp.	[23]
De Los Rios,et al 2018	Distilled- $\text{H}_2\text{O}$	$\text{Al}_2\text{O}_3$	10 at 3% vol.con	Exp.	[24]

As it can be seen from Figure 1 [25],  $\text{Al}_2\text{O}_3$  is the most applicable nanoparticle among researchers since 41% of studies use it in the studies, followed by  $\text{CuO}$ ,  $\text{TiO}_2$ , etc. Both metallic and non-metallic nanoparticles can be dispersed into the base fluid at a different volumetric concentration ranging from 0.01%–6% [26-28].

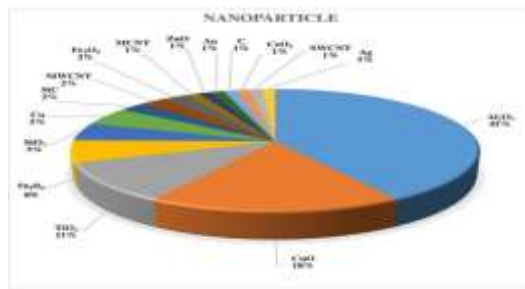


Figure 1: Share of different nanoparticles on the studies concerning PTSC enhancement using Nano-fluids [25].

## 2. The Methodology of Structure Work

### I. Helical coiled receiver tube

The presented PTSC system has been improved by using a modified solar receiver, constructed in the form of coiled helical tube mounted on the focal line of the concentrator trough. Figure 2 shows a cut-away view sketch of the helical coil. The helical coil was manufactured using a bending process to a copper pipe with length  $L_p$  diameter  $D_p$ , and thickness  $\delta_p$ . The coil has dimensions of a length  $L$  which is approximately equal to the length of the collector, diameter  $d$ , and pitch  $P$ . The coil pitch may be defined as the spacing between consecutive coil turns (measured from the center to center), adjusted here with  $P = 1.8 D_p$  [29]. The helical coil tube had been inserted in a smooth glass tube with length  $L_g$ , thickness  $\delta_g$ , and diameter  $D_g$ . The following analysis considers the dimensional and operating parameters needed to construct the required coiled tube, which are listed in Table 1. The coil pipe length  $L_p$  could be determined according to Eq.1 [29]. Initially, this length is needed to form a helical coil with turns of  $n = 116$ , a diameter of  $d=41\text{mm}$ , and an average pitch of approximately 10 mm as an initial value:

$$L = n\sqrt{\pi(d)^2 + p^2} \tag{1}$$

A copper pipe had been procured from the native markets of Baghdad city, has a length  $L_p$  of 15.24 m, diameter  $D_p$  of 6.mm, and thickness  $\delta_p$  0.6 mm, could be used to form a helically coiled tube, with length  $L$  of 1835 mm depending on the length of the collector, number of coil turns  $n$  of 116, mean coil diameter  $d$  of 41mm, by using bending process with a pitch coil of  $P$ . The helical coil is covered with a thin coat of heat resistant black color paint and to minimize the heat losses of the PTSC, a glass tube was used to cover the absorber helical receiver tube. All the helical coil receiver tube specifications are in Table 2.

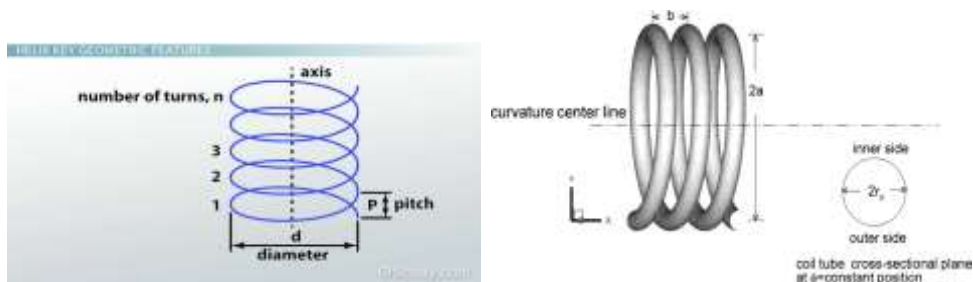


Figure 2: Basic geometry of the helical tube [29]

### II. Parabolic trough solar collector

PTSC system has major component viz. reflector, receiver, support structure, working fluid circulation system and manual tracking system was adopted in this project to reduce overall cost. Construction of the PTSC is modified [30] to application in this experimental work. Detailed picture showing various components in Figures 3a and 3b. The reflector was designed according to a Parabola Calculator 2.1 a freeware program available to calculate aperture area, focal length, exact location on receiver tube and depth of parabolic trough, a commercially available stainless steel sheet with dimensions of (1755 length  $\times$  1000mm width  $\times$  1mm thickness) had been used. Support

structure builder using steel to provide strong mechanical support during high wind speed and harsh environmental conditions. Table 2 contains all the dimensional specifications of the PTSC and other parameters.

**Table 2: Specification of parabolic reflector, helical receiver and glass cover tube**

Parabolic reflector		Helical coiled tube receiver		Glass tube	
Material	stainless steel	Material	99.9% Copper	Material	Boro-silicate glass
Aperture area	1.755 m <sup>2</sup>	thermal conductivity	401 W/mK	Length of glass tube	1.830 m
Aperture width	1 m	Absorption coeff. of coated paint	0.9	Diameter of glass tube	0.058 m
Focal length	0.25 m	coil diameter, d	0.041 m	Thickness of glass tube	0.0001m
thickness	0.001 m	helix length, L	1.835 m		
rim angle	90°	coil pitch, p	0.01m	absorptance	> 92%
concentration ratio	17	no. of coil turns, Nc	116	transmissivity	> 0.95
height	0.25 m	pipe dimension, L <sub>p</sub> * D <sub>p</sub> *t <sub>p</sub>	15.240*0.006 *0.0006 m		
Reflectivity	0.93				



**Figure 3a: Helical coil tube**



**Figure 3b: PTSC system**

### III. Tracking mechanism

A manual solar tracking mechanism was used by mode two-axis tracking of the PTSC system, in this mode, the collector follows both of the sun's changing altitude and azimuth. The mechanical system includes the main structure that supports the solar collector, providing two degrees of freedom (the movement in two directions). A lightweight steel structure was built to provide strong mechanical support against high wind speed and harsh environmental conditions. The mechanical system consists of a fixed part and moving part. The fixed part is very important to fix the PTSC system, called the base. The moving part accomplishes two actions (axial and tilting motion), the axial motion to move the PTSC from east to west to track the sun rays and the tilting motion to move the PTSC upward and downward [31], Figure 4. The tracking mechanism must be reliable and capable to follow

the sun with a certain degree of accuracy, which is depending on the angle of acceptance of the collector.



Figure 4: Manual mechanism tracking

### 3. Nano-fluid

#### I. Nano-fluid Preparation

Before preparing the Nano-fluids, it is very necessary to measure the weight of SiO<sub>2</sub> nanoparticles required in water for varying concentration. This is done by employing the typical expression [25].

$$\varphi \% = \left[ \frac{\varphi_{np}}{\varphi_{np} + \varphi_{bf}} \right] * 100 = \left[ \frac{\frac{W_{np}}{\rho_{np}}}{\frac{W_{np}}{\rho_{np}} + \frac{W_{bf}}{\rho_{bf}}} \right] * 100 \quad (2)$$

The volumetric concentration ( $\varphi$ ) %, weight and density with subscripts (np- nanoparticles and bf- base fluid). The weights of nanoparticles are measured in grams by using the accurate digital balance in Figure 5a. It is necessary to mix 2.46, 5.55 and 9.51gm of SiO<sub>2</sub> in 1000 ml of distilled water in order to make the volumetric concentration ( $\varphi$ ) % of 0.1%, 0.2%, and 0.3%, respectively. Now, stirring is done by putting a small amount of SiO<sub>2</sub> nanoparticles in 1000 ml of distilled water to make the volumetric concentration, continuously for about 30 minutes on the magnetic stirrer with hot plate system, Figure 5b. The solution then put on the sonicator Figure 5c, and sonication is done for three hours to increase stability and dispersed of SiO<sub>2</sub> in H<sub>2</sub>O. Figure 6 shows the prepared sample of 0.1%, 0.2%, and 0.3% vol.conc.SiO<sub>2</sub>-H<sub>2</sub>O, respectively.



Figure 5: a- Digital balance

b- Magnetic stirrer with hot plate

c- Ultra sonicator





Figure 6: Nano fluid SiO<sub>2</sub>-H<sub>2</sub>O vol.conc. A- 0.1%, B- 0.2% and C-0.3%

II. Thermo physical Properties of the Nano-fluid SiO<sub>2</sub>-H<sub>2</sub>O

The Thermo physical properties of the Nano-fluid like, density ρ<sub>nf</sub>, specific heat C<sub>p,nf</sub>, thermal conductivity k<sub>nf</sub> and dynamic viscosity μ<sub>nf</sub> [26, 27]. Specifications of thermo physical properties of the Nano fluid listed in Table 3, according to the following equations:

$$\rho_{nf} = (1 - \phi)\rho_{bf} + \phi \rho_{np} \tag{3}$$

$$C_{p,nf} = \frac{(1-\phi)\rho_{bf}c_{bf} + \phi \rho_{np}c_{np}}{\rho_{nf}} \tag{4}$$

$$K_{nf} = K_{bf} \left[ \frac{K_{np} + 2 K_{bf} + 2 \phi (K_{np} - K_{bf})}{K_{np} + 2 K_{bf} - \phi (K_{np} - K_{bf})} \right] \tag{5}$$

$$\mu_{nf} = \frac{\mu_{bf}}{(1-\phi)^{2.5}} \tag{6}$$

Table 3: Thermophysical properties of water, nanoparticale and nanofluid

Thermo physical properties	H <sub>2</sub> O	SiO <sub>2</sub>	SiO <sub>2</sub> -H <sub>2</sub> O (0.1%)	(SiO <sub>2</sub> -H <sub>2</sub> O) (0.2%)	(SiO <sub>2</sub> -H <sub>2</sub> O) (0.3%)
Density (kg/m <sup>3</sup> )	1000	2220	1122	1244	1366
Specific heat (J/kg.K)	4187	745	3433	2966	2514
Thermal conductivity (W/m.K)	0.667	1.4	0.722	0.780	0.842
Viscosity ( m <sup>2</sup> /s)	0.415e-6	-	0.471e-6	0.725e-6	1.012e-6

4. Experimental Setup

I. Testing Rig

The experiments were carried out during April and May 2019 under Baghdad climate conditions (of latitude 33.3° North, of longitude 44.4° East). The tests were carried out around noon on some clear sky days at local time from 11AM to 13 PM. This time period had been divided into eight time intervals 15 minute each and the PTSC tilt angle was 33°. Figure 7.

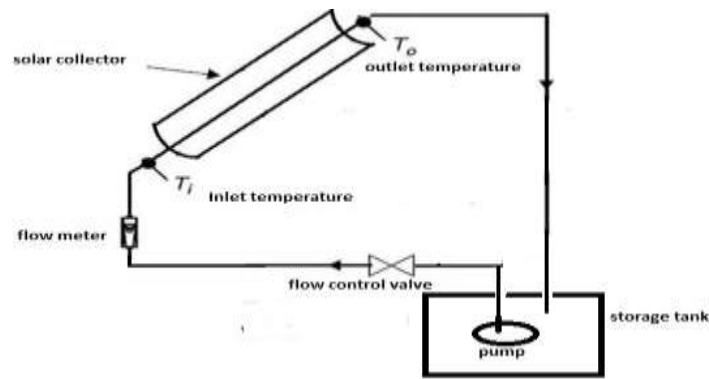


Figure 7: Schematic diagram for the test rig

The performance of the PTSC was tested with a volume fraction of (0.1%, 0.2%, and 0.3%) SiO<sub>2</sub>-H<sub>2</sub>O Nano-fluid and varying flow rate 100 l/h, 150 l/h and 200 l/h. A Thermometer to sense the inlet and outlet temperature, ball valve for varying the volume flow rate with a flow meter, storage tank is made up of plastic and was insulated with the capacity of 10 liter, A healthy insulation utilized on the piping system for preventing the heat loss produced from working Nano-fluid, A 18 W pump was installed inside the tank to avoid the settling of the nanoparticles and to circulate the water through helical receiver tube and the pipes at a certain height, solar meter device was used. The solar collector had been manually pointed to track the sun in a two-axis direction.

## II. Thermal performance

Experimental tests conducted to determine the thermal efficiency of PTSC at near-normal steady state conditions. The tests were performed following the ASHRAE Standard 93-1986 [28]. The efficiency curves are obtained based on the executed experiments. Basic measurements are inlet  $T_i$ , outlet  $T_o$  and ambient  $T_a$  temperature, direct beam solar irradiance  $G_T$ , flow mass of the fluid  $m^*$ , and aperture area  $A_C$ . The specific heat  $C_p$  is obtained depending on the fluid used to characterize the collector Eq.7. Also that useful heat gain could also be indicated in term of the energy absorbed by absorbent and those lost from the absorber Eq.8 with applied the removal factor  $F_R$ , transmittance factor  $\tau$ , glass absorptance factor  $\alpha$  and overall loss coefficient of solar collector  $U_L$ , as given by Eq.8. [33]. According to combined Eqs. (7-13) provides the basis for simulation models [28, 29]:

$$Q_u = m^* C_p (T_o - T_i) \quad (7)$$

$$Q_u = F_R [G_T (\alpha\tau) A_C - U_L A_C (T_i - T_a)] \quad (8)$$

$$F_R = \frac{m^* C_p (T_i - T_a)}{[G_T (\alpha\tau) A_C - U_L A_C (T_i - T_a)]} \quad (9)$$

$$\eta = \frac{Q_u}{A_C G_T} \quad (10)$$

$$\eta = \frac{F_R [G_T (\alpha\tau) A_C - U_L A_C (T_i - T_a)]}{A_C G_T} \quad (11)$$

$$\eta = F_R \left[ \alpha\tau - \frac{U_L [T_i - T_a]}{G_T} \right] \quad (12)$$

$$\eta = F_R (\alpha\tau) - F_R U_L \left[ \frac{[T_i - T_a]}{G_T} \right] \quad (13)$$

The experimental results are demonstrated as graphs indicating the PTSC efficiency against the heat loss parameter  $[(T_i - T_a)/G_T]$ . Therefore, the efficiency is expressed from Eq. 13, as a

straight-line [35]. From the averaged data plotted against x-axis  $(T_i - T_a)/G_T$ , this line intersects the y-axis  $F_R(\tau\alpha)$ . The efficiency of the Collector reaches its peak value at  $(T_i = T_a)$ . The factor  $F_R(\tau\alpha)$  is called “energy absorbed factor”. The straight line slop is equal to the factor  $F_{RUL}$  and called “energy removal factor”.

**5. Results and Discussion**

The thermal efficiency results of the PTSC are discussed in four sections: First part by with Distilled- $H_2O$  as a working fluid. Second part is represented by utilizing the  $SiO_2-H_2O$  Nano-fluid as a work fluid. Third part discusses the impact of Nano-fluid volume fraction. The fourth part deals with the influence of the flow rate.

*I. Distilled- $H_2O$*

Figure 8 illustrates of the PTSC efficiency and reduced temperature difference parameter for distilled  $H_2O$  at varying flow rate 100, 150 and 200 l/h. From the experimental results, the performance curves of the solar collectors under the ASHRAE Standard with distilled  $H_2O$  at flow rate 100,150, and 200 l/h, respectively are given. It is found that thermal solar characteristics values of energy absorbed factor  $F_R(\tau\alpha)$  are 0.641, 0.654, and 0.668, respectively. Also the energy removal factor  $- F_{RUL}$  are 8.23, 8.44 and 8.59  $W/m^2.k$ , respectively. It is seen that both  $F_R(\tau\alpha)$  and  $F_{RUL}$  are increased with the flow rate increase. The PTSC efficiency for 200 l/h is highest and was 66.8 %.

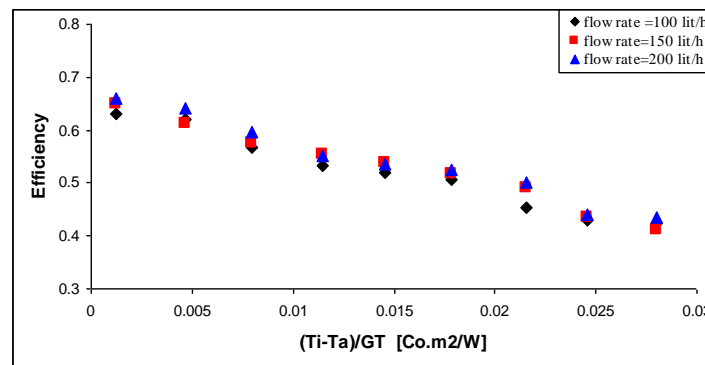


**Figure 8: Efficiency of solar collector using distilled water only**

*II.  $SiO_2-H_2O$*

Experimental observation of the PTSC was administrated in Table 4 to find out a variation in collector efficiency at varying flow rates (100,150 and 200 l/h) at different  $\phi$  % (0.1, 0.2 and 0.3 %). Figures 9-11 illustrate the thermal efficiency of PTSC and reduced  $(T_i - T_a)/G_T$  at the  $\phi$ % (0.1, 0.2 and 0.3 %). From the observed data, the efficiency of PTSC is inversely proportional to  $(T_i - T_a)/G_T$  at different  $\phi$ %. It means collector efficiency increases with decreasing  $(T_i - T_a)/G_T$ . Experimental results show that the maximum efficiency was observed up to 76.6% at an optimum particle volume concentration of 0.3% and flow rate 200 l/h, so, the heat loss parameter should be minimized to enhance PTSC efficiency. Also the Brownian movement between the nanoparticles of the work fluid is a prime factor for thermal conductivity enhancement. So, the rate of heat transfer in the solar collector will rise via particle loading [39].

**Table 4: Parameters of  $F_R(\tau\alpha)$  and  $- F_{RUL}$  for water &  $SiO_2$ -water nano-fluid at different volume fraction and flow rates**

Coolant	( $\phi$ %) vol	$m^*$ l/h	$F_R(\tau\alpha)$	$- F_{RUL}$
Water	-	100	0.6413	8.2302
	-	150	0.6545	8.4486
	-	200	0.6689	8.5918
Nano fluid	0.1	100	0.6840	9.0896



(SiO <sub>2</sub> +DW)		150	0.7004	9.4031
		200	0.7193	10.1220
Nano fluid (SiO <sub>2</sub> +DW)	0.2	100	0.7022	9.6028
		150	0.7178	9.8966
		200	0.7403	10.429
Nano fluid (SiO <sub>2</sub> +DW)	0.3	100	0.7175	9.9219
		150	0.7416	10.298
		200	0.7667	11.1190

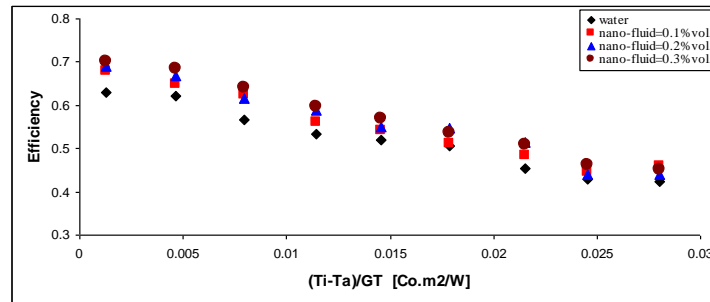


Figure 9: Solar collector efficiency using SiO<sub>2</sub>-water nanofluid at flow rate 100 l/h

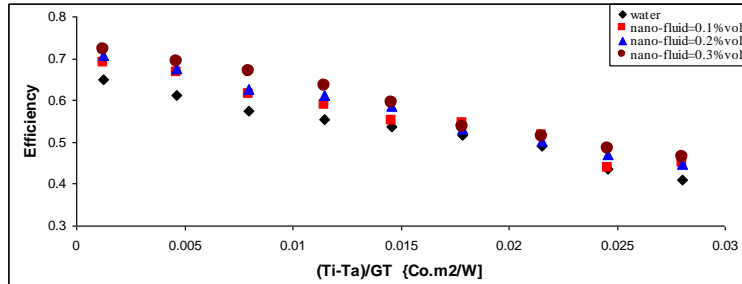


Figure 10: Solar collector efficiency using SiO<sub>2</sub>-water nanofluid at flow rate 150 l/h

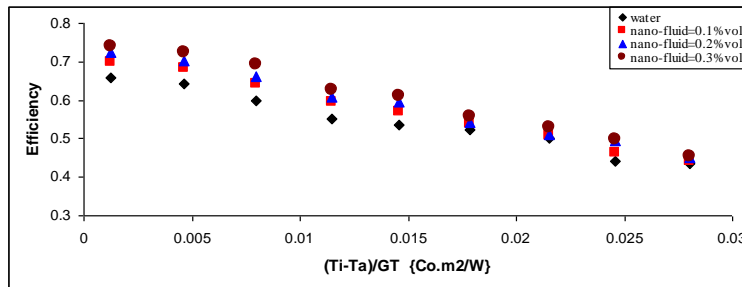


Figure 11: Solar collector efficiency using SiO<sub>2</sub>-water nanofluid at flow rate 200 l/h

### III. Volume fraction and Efficiency

The thermal efficiency of the PTSC system with SiO<sub>2</sub>-H<sub>2</sub>O Nano-fluid has a large depends on ( $\varphi$ ). This conclusion can detect by finding the value of the energy absorbed factor  $F_R(\tau\alpha)$  and the energy removal factor  $F_{RUL}$  for SiO<sub>2</sub>-H<sub>2</sub>O Nano fluid in Table 3. The Figures 12-14 present the solar collector efficiency with using volume fraction of (0.1%, 0.2% and 0.3%) of SiO<sub>2</sub> at different flow rates of 100 l/h, 150 l/h and 200 l/h. The changes of  $F_R(\tau\alpha)$  and  $F_{RUL}$  values at different rates of volume fraction and mass flow are mentioned previously here they are not repeated. Based on present results, it is found that both values of  $F_R(\tau\alpha)$  and  $F_{RUL}$  for all studied mass flow rates more than the values for water. Generally, the energy absorbed factor  $F_R(\tau\alpha)$  and the energy removal  $F_{RUL}$  values are increased as the flow rate rates and volume fraction rise . From, Figure 12, for the flow rate of 100l/h,  $F_R(\tau\alpha)$  values for SiO<sub>2</sub>-H<sub>2</sub> O nano-fluid is more than water by 6.6%, 7.0% and 7.5% for  $\varphi$  (0.1%, 0.2% and 0.3%), respectively. Although ( $F_{RUL}$ ), values for SiO<sub>2</sub>-H<sub>2</sub>O nano-fluid rise by 10.4%, 11.2% and 17.8% for  $\varphi$ % (0.1%, 0.2% and 0.3%) respect to water. Based on, Figure 13, going up in values of  $F_R(\tau\alpha)$  at mass flow rates of 150l/h is 9.4%, 9.6%, and 10.6% at  $\varphi$  of (0.1%, 0.2%, and 0.3%), respectively and increasing in values of  $F_{RUL}$  is 16.6%, 17.1%, and 21.3% for a  $\varphi$  of (0.1%, 0.2% and 0.3%), respectively comparing to water. Figure 14 showed values of  $F_R(\tau\alpha)$  and  $F_{RUL}$  for the mass flow rate of 200l/h. Values of  $F_R(\tau\alpha)$  is raised by 11.8%, 13.3% and 14.6% for  $\varphi$  (0.1%, 0.2%, and 0.3%), respectively. It is observed that the gain in values of  $F_{RUL}$  for SiO<sub>2</sub>-H<sub>2</sub>O nano-fluid increased by 20.5%, 21.8% and 29.4% for  $\varphi$  (0.1%, 0.2% and 0.3%) respect to water. The thermal efficiency lines intersect each other. It is seen that the PTSC efficiency increases with the flow rate for a wide range of the heat loss parameter,  $[(T_i-T_a)/GT]$  and varying different nanoparticle concentrations. Enhancing the efficiency of the PTSC causing by rising the flow rate is higher at the maximum concentrations; this may be due to the Brownian movement increase in nano-fluids, thereby increasing the discontinuity in the boundary layer. Relative movement and diffusion of nanoparticles near the tube wall will cause a fast heat transfer from the wall to the nano-fluid. This means that increasing the nanoparticle concentrations will amplify the mechanisms responsible for enhancing the heat transfer. So, generally, the nano-fluids at higher volume concentrations have larger values of convective heat transfer coefficients.

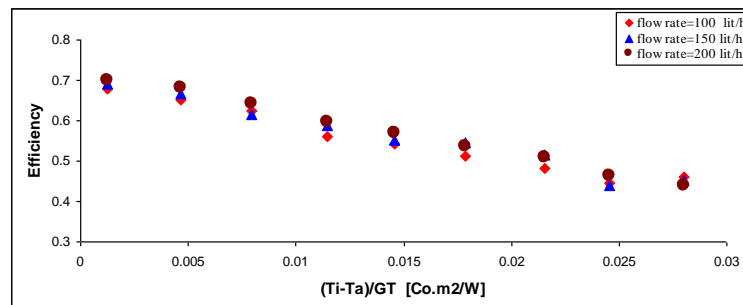


Figure 12: Solar collector efficiency using  $\varphi = 0.1\%$  of SiO<sub>2</sub> at different flow rates

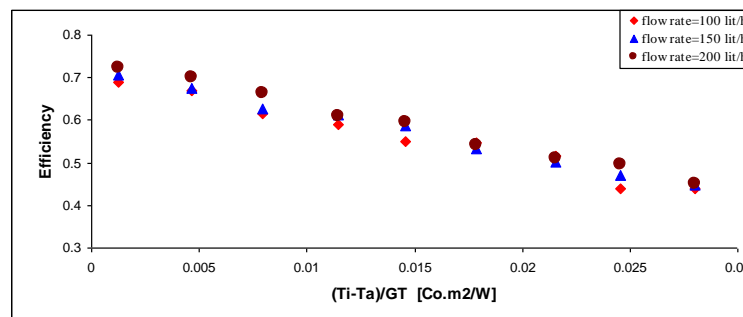
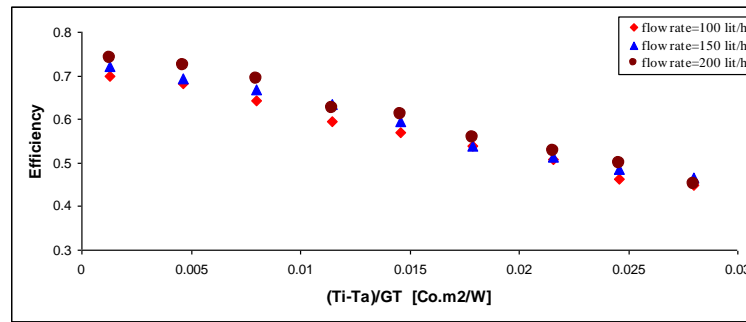


Figure 13: Solar collector efficiency using  $\varphi = 0.2\%$  of SiO<sub>2</sub> at different flow rates



**Figure 14: Solar collector efficiency using  $\phi = 0.3\%$  of  $\text{SiO}_2$  at different flow rates**

#### IV. Flow rate and Efficiency

Figure 15 shows the relation between collector efficiency and flow rates of the fluids at varying of the  $\phi\%$ . In this graph, the thermal efficiency of the PTSC using  $\text{H}_2\text{O}$  and  $\text{SiO}_2\text{-H}_2\text{O}$ , flow rate fluid 100, 150 and 200 l/h and the  $\phi\%$  (0.1, 0.2, and 0.3 %). The results demonstration that the maximum efficiency of the PTSC was observed up to 76.6 % at an optimum value of mass flow rate 200 l/h and particle concentration 0.3%. The explanation of this behavior is that when the flow rate of working fluid increases, the velocity and Reynolds number of the work fluid increases too. Also, heat transfer will increase [37, 38]. Therefore, the motion rate, especially the Brownian motion and the turbulence of the particles in the nano-fluid are increasing proportional to the flow rate and velocity of the nano-fluid. Comparing to using water, the movement of the nanoparticles in the nano-fluid produces a larger heat transfer and a subsequent dramatic rise in the system thermal efficiency [39, 40].

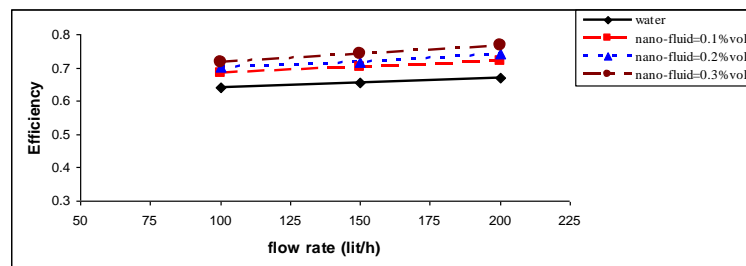


**Figure 15: Flow rate and efficiency at different  $\phi\%$  of nano-fluid ( $\text{SiO}_2 + \text{H}_2\text{O}$ )**

## 6. Conclusions

A study had been experimentally carried out to present the thermal efficiency of the PTSC.  $\text{SiO}_2\text{-H}_2\text{O}$  as working fluid is used. Different values of  $\phi$  of 0.1%, 0.2%, and 0.3% were examined at three flow rates of 100 l/h, 150 l/h, and 200 l/h. The experiments and results clarify that using  $\text{SiO}_2\text{-H}_2\text{O}$  nano-fluid increases the efficiency of PTSC more than utilizing water only. The results showed that the maximum thermal efficiency with heat loss parameter,  $(T_i - T_a)/G_T = 0$  was 0.766 at  $\phi$  value of 0.3 % and flow rate of 200 l/h. The highest rise in the energy absorbed energy factor  $F_R(\tau\alpha)$  was 14.6% at volume fraction 0.3% and a flow rate 200 l/h, so this case has the maximum increase in efficiency compared to water. The maximum increase in FRUL was at a volume fraction of 0.3% and flow rate of 200 l/h. The changes in energy absorbed factor  $F_R(\tau\alpha)$  vary from 11.8% to 14.6% and in energy removal factor FRUL, vary from 20.5% to 29.4% compared to water as working fluid. The efficiency of collector is directly proportional with both volume fraction of nanoparticles and flow rate. Finally, the proposed PTSC based on helical coil tube receiver and nano-fluids is a new work and may be enhanced for more applications.

## 7. Future Scope

Very limited experimental works have been done on the PTSC, so it has wide scope in future. In the present experimental work, a lot of things which are not taken in account can be employed in future to enhance the performance of the PTSC based on nano-fluid and helical receiver tube some of these are:

- i. Varying material and the dimension of helical receiver tube
- ii. Pressure, velocity, and profile motion flow inside helical receiver.
- iii. Varying of nanoparticles materials and nano-fluids volumetric concentration.
- iv. Air as a working median instead of using nano-fluid with the help of blower.

**References**

- [1] R. Loni, E. AskariAsli-ardeh, B. Ghobadian, A.B. Kasaeian, Sh. Gorjian, "Thermodynamic analysis of a solar dish receiver using different Nano fluids," *Energy*, vol. 133, pp. 749-760, 2017.
- [2] A. G. Fernandez, H. Galleguillos, E. Fuentealba, F. J. Perez, "Thermal characterization of HITEC molten salt for energy storage in solar linear concentrated technology," *Journal of Thermal Analysis and Calorimetry*, vol. 5, no. 122-1, pp. 3-9, 2015.
- [3] E. Mathioulakis, E. Papanicolaou, V. Belessiotis, "Optical performance and instantaneous efficiency calculation of linear Fresnel solar collectors," *International Journal of Energy Research*, pp. 1-15, 2017.
- [4] E. Bellos, C. Tzivanidis, A. Papadopoulos, "Enhancing the performance of a linear Fresnel reflector using Nano fluids and internal finned absorber," *Journal of Thermal Analysis and Calorimetry*, 2018.
- [5] W. Fuqiang, C. Ziming, T. Jianyu, Y. Yuan, S. Yong, L. Linhua, "Progress in concentrated solar power technology with parabolic trough collector system: A comprehensive review," In *Renewable and Sustainable Energy Reviews*, vol. 79, pp. 1314-1328, 2017.
- [6] H.M. Sandeep, U.C. Arunachala, "Solar parabolic trough collectors: A review on heat transfer augmentation techniques," *Renewable and Sustainable Energy Reviews*, vol. 69, pp. 1218-1231, 2017.
- [7] Z. Huang, Z.-Y. Li, G.-L. Yu, W.-Q. Tao, "Numerical investigations on fully developed mixed turbulent convection in dimpled parabolic trough receiver tubes," *Applied Thermal Engineering*, vol. 114, pp. 1287-1299, 2017.
- [8] G. Xiangtao, W. Fuqiang, W. Haiyan, T. Jianyu, L. Qingzhi, H. Huaizhi, "Heat transfer enhancement analysis of tube receiver for parabolic trough solar collector with pin fin arrays inserting," *Solar Energy*, vol. 144, pp. 185-202, 2017.
- [9] E. Bellos, C. Tzivanidis, D. Tsimpanos, "Multi-criteria evaluation of parabolic trough collector with internally finned absorbers," *Applied Energy*, vol. 205, pp. 540-561, 2017.
- [10] A. Mwesigye, T. Bello-Ochende, J.P. Meyer, "Heat transfer and entropy generation in a parabolic trough receiver with wall-detached twisted tape inserts," *International Journal of Thermal Sciences*, vol. 99, pp. 238-257, 2016.
- [11] B. Bhanvase, S.D. Sayankar, A. Kapre, P.J. Fule, S.H. Sonawane, "Experimental investigation on intensified convective heat transfer coefficient of water based PANI Nano fluid in vertical helical coiled heat exchanger," *Applied Thermal Engineering*, vol. 128, pp. 134-140, 2018.
- [12] M. Bahiraei, RezaRahmani, Ali Yaghoobi, Erfan Khodabandeh, Ramin Mashayekhi, Mohammad Amani, "Recent research contributions concerning use of nanofluids in heat exchangers: A critical review," *Applied Thermal Engineering*, vol. 133, no. 137, pp. 137-159, 2018.
- [13] S. Kumar, K Vasudev Karanth, "Numerical analysis of a helical coiled heat exchanger using CFD," *Int. Journal of Thermal Technologies*, vol.3, pp. 126-130, 2013.
- [14] A. Alimoradi, "Study of thermal effectiveness and its relation with NTU in shell and helically coiled tube heat exchanger," *Elsevier Case Studies in Thermal Engineering*, vol.9, pp. 100-107, 2017.
- [15] R. Gupta, S. Kalmegh, P. Warghade, K. Padghan, "Experimental study on helical tube heat exchanger by varying cross section using nanoParticles," *IRJET*, vol.5, 6, pp. 2746-2749, 2018.
- [16] S. U. Choi, J. Eastman, "Enhancing thermal conductivity of fluids with nanoparticles," Argonne National Lab, IL (United States), 1995.
- [17] O. Mahian, A. Kianifar, A.Z. Sahin, S. Wongwises, "Entropy generation during Al<sub>2</sub>O<sub>3</sub>/water nano fluid flow in a solar collector: effects of tube roughness, nanoparticle size, and different thermophysical models," *Int. Journal of Heat and Mass Transfer*, vol. 78, pp. 64-75, 2014.
- [18] K. Sunil, L. Kundan, S. Sumeet, "Performance evaluation of a Nano fluid based parabolic solar collector-an experimental study," In *Proceedings of twelfth IRF international conference*, Chennai, India, pp. 29-35, 2014.
- [19] S. Chaudhari, P. V. Walke, U. S. Wankhede, R. S. Shelke, "An experimental investigation of a nano fluid (Al<sub>2</sub>O<sub>3</sub>+H<sub>2</sub>O) based parabolic trough solar collectors," *Br. J. Appl. Sci. Technol.* vol. 9, pp. 551-557, 2015.

- [20] J. Subramani, P.K. Nagarajan, S. Wongwises, S.A. El-Agouz, R. Sathyamurthya, "Experimental study on the thermal performance and heat transfer characteristics of solar parabolic trough collector using  $\text{Al}_2\text{O}_3$  nanofluids," *Environmental Progress & Sustainable Energy*, vol. 10, no. 1002, 2017.
- [21] M.A. Rehan, M. Ali, N.A. Sheikh, M.S. Khalil, G.Q. Chaudhary, T. ur Rashid, M. Shehryar, "Experimental performance analysis of low concentration ratio solar parabolic trough collectors with nanofluids in winter conditions," *Renewable Energy*, vol. 118, pp. 742-751, 2018.
- [22] J. Subramani, P.K. Nagarajan, O. Mahian, R. Sathyamurthy, "Efficiency and heat transfer improvements in a parabolic trough solar collector using  $\text{TiO}_2$  nanofluids under turbulent flow regime," *Renewable Energy*, vol. 10, no. 1016, 2017.
- [23] A. Deep Sheel, Arun Kumar Tiwari and Shailendra Sinha, "Analysis of parabolic trough solar collector using  $\text{TiO}_2$ /water nano fluid," *International Journal Mechanical Technology*, vol.9, no. 9, pp. 1094-1102, 2018.
- [24] D. Rios, M.S.B., Rivera-Solorio, C.I., García-Cuéllar, A.J., "Thermal performance of a parabolic trough linear collector using  $\text{Al}_2\text{O}_3/\text{H}_2\text{O}$  nanofluids," *Renew. Energy*, vol. 122, pp. 665-673, 2018.
- [25] E. Bellos, E. Tzivanidis, C., "A review of concentrating solar thermal collectors with and without nanofluids," *J. Thermal Anal. Calorim*, pp. 1-24, 2018.
- [26] E. Bello, Tzivanidis, C. Tsimpoukis, D., "Enhancing the performance of parabolic trough collectors using nanofluids and turbulators," *Renew. Sustain. Energy*, vol. 91, pp. 358-375, 2018.
- [27] S.Kandwal, Lal, K.G., "An experimental investigation into nanofluids ( $\text{CuO}-\text{H}_2\text{O}$  &  $\text{CuO}$ -ethylene glycol) based parabolic solar collector," MSc. Thesis, Thapar institute, 2015.
- [28] S. Kapil, and Kundan Guide Lal., "An experimental investigation into the performance of a nanofluid based concentrating parabolic solar collector (NCPSC)," PhD diss., Thapar institute, 2014.
- [29] R. Patil, Shende B.W. Ghosh, P.K. , "Designing a helical-coil heat exchanger," *Chem. Eng.*, vol. 13, pp. 85-88, 1982.
- [30] M. Laith M., "Design and Implementation of high efficiency thermal system using plc microcontroller," MSc. Thesis, University of Technology, Baghdad, 2017.
- [31] S.Tami, J.A. Mohammed, Laith M. Reda, "Design and implementation of an automatic control for two-axis tracking system for applications of concentrated solar thermal power," *Al-Khwarizmi Engineering Journal*, vol.14, no. 4, pp. 54-63, 2018.
- [32] M. Chang, H. S. liu, C. Y. Tai, "Preparation of copper oxide nanoparticles and its application in Nano fluid, powder technology," vol. 207, pp. 378-386, 2011.
- [33] T. yousefi, F. Veysi, E. Shajaeizadeh, S. Zinadinis, "An experimental investigation on effect of  $\text{Al}_2\text{O}_3-\text{H}_2\text{O}$  nano fluid on the efficiency of flat-plate solar collector," *Renewable energy*, vol.39, pp. 293-298, 2012.
- [34] F.S. Javadi, S. Sadeghipour, R.. Saidur, G. Boroumandjazi, B. Rahmati, M. M. Eilas M. R. Sohel, "The effects of Nano fluid on thermophysical properties and heat transfer characteristics of a plate heat exchanger," *International Communications in Heat and Mass Transfer*, vol.44, pp. 58-63, 2013.
- [35] ASHRAE Standard 93-86, "Methods of testing and determine the thermal performance of solar collectors," ASHRAE, Atlanta, 2003.
- [36] Duffie, J.A., Beckman, W. A., "Solar engineering of thermal processes," Wiley publication, 1991.
- [37] C. Cristofari, G. Notton, P. Poggi, A. Louche, "Modeling and performance of a copolymer solar water heating collector," *Solar Energy*, vol. 72, pp. 99-112, 2002.
- [38] A. Mintsa, M. Medale, C. Abid, "Optimization of the design of a polymer flat plate solar collector," *Solar Energy*, vol. 87, pp. 64-75, 2013.
- [39] Y. Xuan, Q. Li, W. Hu, "Aggregation structure and thermal conductivity of nanofluids," *AIChE Journal*, vol. 49, pp. 1038-1043, 2003.
- [40] S. Salavati Meibodi, Ali Kianifar, Hamid Niazmand, Omid Mahian, and Somchai Wongwises, "Experimental investigation on the thermal efficiency and performance characteristics of a flat plate solar collector using  $\text{SiO}_2/\text{EG}$ -water nanofluids," *Int. Communications in Heat and Mass Transfer*, vol. 65, pp.71-75, 2015.